High-power photonic-bandgap fiber laser

Sébastien Février,[1,*] Dmitry D. Gaponov,[1,2] Philippe Roy,[1] Mikhail E. Likhachev,[2] Sergei L. Semjonov,[2] Mikhail M. Bubnov,[2] Evgeny M. Dianov,[2] Mikhail Yu. Yashkov,[3] Vladimir F. Khopin,[3] Mikhail Yu. Salganskii,[3] and Aleksei N. Guryanov[3]

[1]*Xlim, UMR 6172 CNRS, University of Limoges 123 Avenue A. Thomas, 87060 Limoges, France*
[2]*Fiber Optics Research Center, 38 Vavilov Street, Moscow 119333, Russia*
[3]*Institute of Chemistry of High Purity Substances, 49 Tropinin Street, Nizhny Novgorod 603950, Russia*
[*]*Corresponding author: sebastien.fevrier@xlim.fr*

Received October 17, 2007; revised March 6, 2008; accepted March 12, 2008;
posted March 25, 2008 (Doc. ID 88643); published April 29, 2008

An original architecture of an active fiber allowing a nearly diffraction-limited beam to be produced is demonstrated. The active medium is a double-clad large-mode-area photonic-bandgap fiber consisting of a 10,000 ppm by weight Yb^{3+}-doped core surrounded by an alternation of high- and low-index layers constituting a cylindrical photonic crystal. The periodic cladding allows the robust propagation of a $\sim 200\ \mu m^2$ fundamental mode and efficiently discriminates against the high-order modes. The M^2 parameter was measured to be 1.17. A high-power cw laser was built exhibiting 80% slope efficiency above threshold. The robust propagation allows the fiber to be tightly bent. Weak incidence on the slope efficiency was observed with wounding radii as small as 6 cm. © 2008 Optical Society of America

OCIS codes: 060.2280, 060.2270.

The fiber laser architecture is becoming a competitor to other solid-state lasers even in the reach for high cw power. One main advantage of fiber lasers is the possibility to reach nearly diffraction-limited beams. However, the increase in the output power is severely limited by the onset of such nonlinear impairments as stimulated scatterings (Brillouin, Raman, and Kerr effects). To increase the threshold of nonlinear effects, large-mode-area (LMA) fibers are routinely used. Scaling of output power up to the kilowatt range has been demonstrated using step-index fibers [1]. By nature, the LMA architecture is obtained at the cost of weakening the waveguidance in the fiber, leading to a strong bend sensitivity. The cost is that the fiber must be straight to avoid any power leakage, forbidding the construction of compact fiber lasers. Moreover, bending results in a reduction of effective area that could lead to detrimental nonlinearities [2].

Solutions based on effectively single-mode fibers were recently proposed. Here, multimode fibers are used. Together with the discrimination of high-order modes (HOMs) by proper curvature of a highly multimode fiber [3], the use of helical-core fiber [4], spun-double-core fiber [5], or gain-guided, index-antiguided fibers [6] are promising techniques.

In this Letter, we propose a novel architecture of fiber laser based on the discrimination of transverse modes obtained in a photonic-bandgap fiber. Obviously, we deal with solid-core bandgap fiber doped with rare-earth ions, e.g., Yb^{3+}. For the solid-core mode to be guided by the bandgap effect, the periodic cladding must be composed of high-index inclusions embedded in a low-index background. Based upon the seminal work of Yeh *et al.* [7], we recently proposed an effectively single-mode LMA photonic-bandgap fiber composed of a low-index core surrounded by a periodic cladding composed of alternating high- and low-n layers [see Fig. 1(a)] [8]. Contrary to the air-core design proposed in [7], our solid-core version needs very few pairs of layers and a low-index contrast to efficiently guide light in the core. For the sake of simplicity, the index of the core is chosen to be equal to that of the pure silica low-n layers. The high-n layers are GeO_2-doped. Such a preform can be made by the modified chemical-vapor deposition (MCVD) process. As the proposed fiber is a leaky waveguide, a trade-off regarding the modes' attenuation coefficients must be found; the first Gaussian mode must exhibit low (<1 dB/m) loss, while the HOMs must exhibit high (>100 dB/m) loss at a specified wavelength. This requirement can be fulfilled by engineering the index profile. Degrees of freedom are core diameter D, lattice constant Λ, thickness d, and index contrast Δn of high-n layers and number N of bilayers. To optimize an index profile we need to choose core diameter as well as the index in each section of the profile. For the high-power fiber laser application, $D > 20\ \mu m$ is chosen. Indices are chosen considering the MCVD process requirements ($\Delta n < 0.05$). At a specified wavelength λ, the radiation must resonate in the core. This leads to a certain value of the mode effective index (n_{e01}) together with the transverse wavenumbers in the ith cladding layer $p_i = k_0\sqrt{n_i^2 - n_{e01}^2}$. Under the quarter-wave stack condition, it is then straightforward to determine Λ and d. Then, the design space reduces to $\{D, \Delta n, N\}$. For such a triplet, attenuation coefficients of LP_{01} and LP_{11} modes are computed using the transfer matrix method. An example of results is shown in Fig. 1(b) for $D = 20\ \mu m$. Obviously, the attenuation coefficients of both modes decrease with N and Δn. A strong discrimination against HOMs will necessitate $\alpha_{11} > 100$ dB/m, while a quasi-lossless propagation of LP_{01} is preferred. Graphically, we can determine that for $D = 20\ \mu m$, $\Delta n = 0.015$ and $N = 3$ are well suited. The bend influence was also computed using a full-vector finite element algorithm. A conformal transformation was applied to simulate the

0146-9592/08/090989-3/$15.00

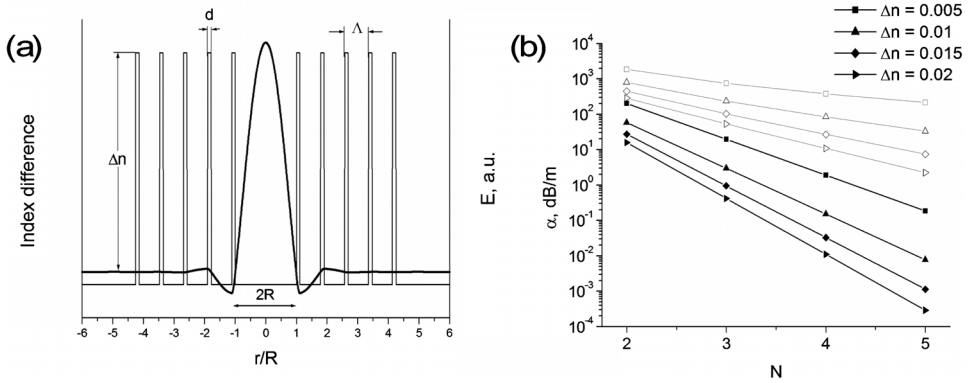

Fig. 1. (Color online) (a) Theoretical refractive index profile of solid-core bandgap fiber. The design space includes the core diameter D, the cladding index contrast Δn, and the number N of bilayers. Also reported is an example of electric field distribution. (b) Attenuation coefficients computed when $D=20$ μm for various Δn in the range (0.005, 0.01, 0.015, 0.02) as functions of N. Hollow symbols, LP_{11}; filled symbols, LP_{01}.

propagation in the bent fiber. A perfectly matched layer was added to evaluate the radiation loss due to bend. The critical bend radius defined as the radius leading to a 3 dB/m loss for the fundamental mode was computed to 8 cm for the proposed design. This bend radius does not affect the effective mode area ($\sim$170 μm^2). A preform was then manufactured and drawn down to a dual-clad fiber.

The index profile of the fabricated fiber is shown in Fig. 2. High-index layers were GeO_2 doped ($\Delta n = 15 \times 10^{-3}$). Highly Yb^{3+} ($\sim$10,000 ppm by weight) core doping was obtained by utilization of metal-organics substances as precursors. The Yb^{3+} absorption reaches 800 dB/m at 976 nm wavelength. The core was doped with Al_2O_3 (to increase solubility of Yb^{3+}) and codoped with F (to cancel index difference). Variations of the core index along radius are due to evaporation of core dopants during preform collapse. These variations could be detrimental. Hence, the mode characteristics (field distribution and confinement loss) were computed in the actual index profile. The periodic cladding behaves as an efficient reflector for the fundamental mode (loss computed to $\sim$1 dB/m) whereas confinement loss for higher-order modes are close to 10 dB/m. Effective area of the fundamental mode is close to 200 μm^2. The fiber was coated with a low-index polymer leading to a cladding numerical aperture close to 0.48.

Although the confinement loss of HOMs is relatively high, these modes could propagate in the fiber. Thus, we observed the transverse field intensity distribution at the output of a short (2 m) piece of fiber in absence of pumping. The wavelength of the launched radiation was 1.064 μm. The launching conditions were changed to observe possible HOMs. Results are shown in inset of Fig. 2. It is obvious that the unpumped fiber is slightly multimode. Launching efficiency of HOMs is rather high. However, the fabricated fiber is to be used as a laser without launched signal radiation. Then, the signal radiation was suppressed, and pump radiation was launched into the outer cladding. Pump light was delivered by a multimode diode laser emitting at 975 nm with pigtail core diameter of 100 μm and NA of 0.22. Thanks to the high Yb^{3+} concentration, the short 2 m long piece of fiber was used. The cavity mirrors were a dichroic mirror with maximum reflectivity at the signal wavelength (Rmax at 1060 nm) and the cleaved output end of the fiber. Pump launching efficiency reached 80%. Laser and remaining pump beams were split at the output by using another dichroic mirror (Rmax at 1060 nm, Tmax at 975 nm). It should be mentioned that any mechanical stresses on the fiber must be avoided when maintaining it on support plates. Indeed applied stress locally disturbs the index profile, and unwanted coupling to ring modes occurs.

First, the transverse distribution of the mode field intensity was observed at the output end of the laser. As shown in Fig. 3(a), the beam profile is representative of a single-mode emission. Thanks to the three-axis translation stage, the input mirror was tilted. HOMs were never excited, evidencing the single-mode behavior of the fabricated fiber when lasing. As pointed out in [9] selective amplification of modes occurs owing to difference in overlap integrals. Characteristics of the first and second modes were computed. The effective indices ($n_{e01}=1.448561$ and $n_{e11}=1.448144$ for a background index equal to that of

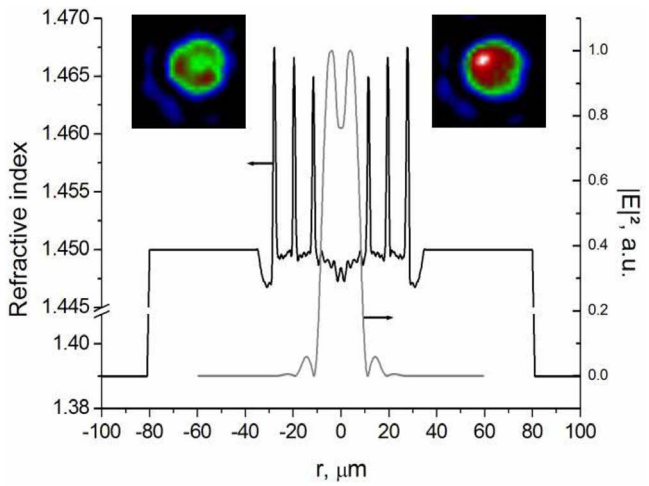

Fig. 2. (Color online) Refractive index profile and computed electric field intensity distribution of considered bandgap fiber at 1064 nm. Inset, intensity distribution observed at the output of a 2 m long piece of fiber without pumping for various launching conditions. $\lambda = 1.064$ μm.

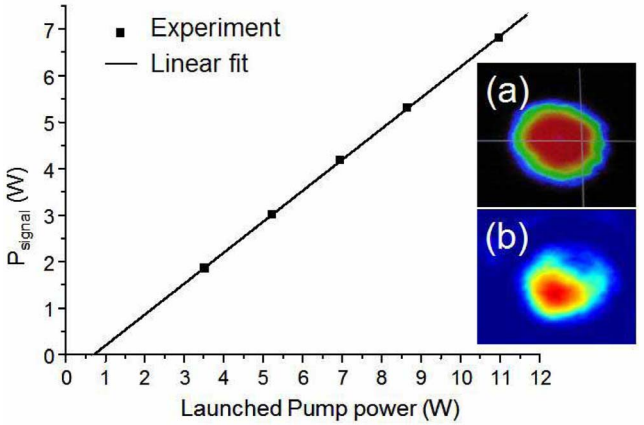

Fig. 3. (Color online) Output power as a function of the launched pump power for the straight fiber. Inset, beam profile observed at the output end of the fiber. (a) Rc = 7.5 cm, three turns; (b) Rc = 2.5 cm, seven turns.

silica n = 1.45) were found to be close to each other, as usually observed in a LMA fiber. The overlap integrals were computed to 87% and 50% for the first and second modes, respectively. The difference is thought to be large enough to explain the observed behavior. Other features related to the spatial beam quality; i.e., effective numerical aperture NA and beam quality factor M^2 were also determined. The NA has been evaluated from the value measured for a very similar but passive fiber [7] and was estimated to be 0.06. The M^2 parameter has been measured by the knife-edge technique and found to be equal to 1.17. Contrary to the step-index fiber (SIF), the mode is entirely confined to the low index core. Consequently, the field distribution follows the Bessel function of first kind and first order (J_0). The M^2 parameter, comparing the generated beam and a purely Gaussian beam, is then slightly higher than that of a SIF.

Then, the output power was measured as a function of the launched pump power for the straight fiber. Results are plotted in Fig. 3. Slope efficiency was measured to 67% with respect to launched power. It is worth noting that the fiber length is too short to efficiently absorb all the pump power. We then evaluated the slope efficiency versus the absorbed pump power. To do so, the absorbed pump power was measured by the cut-back technique between the fiber output and a 5 cm long piece of fiber at the input. This technique implies an uncertainty due to the pump power absorbed in the 5 cm long piece of fiber. However, under such high pump power, the medium is almost entirely inverted and becomes transparent to the incident pump power. Thus, uncertainty is evaluated to be on the order of 1%. When considering the absorbed pump power, the slope efficiency is (80 ± 1)%. Further, pump absorption can be improved, for instance, by using D-shape inner cladding.

Then, bend influence on lasing was characterized. For a reasonable radius (Rc = 7.5 cm) and three turns, there is no influence on beam shape [see Fig. 3(a)]. Even for a very tight bend (Rc = 2.5 cm, seven turns), HOMs were never excited as shown in Fig. 3(b). On the other hand, we observed the bend-induced field distortion. Such distortion occurs at a bend radius corresponding to high additional loss as shown by the increase of the lasing threshold (measured to be 6 W), that is to say at a bend radius not corresponding to an efficient operation of the laser. Bend-induced nonlinearities are thus not expected in this kind of fiber. At 6 cm bend radius, neither influence on the slope efficiency nor on the lasing threshold were observed.

In conclusion, an active solid-core photonic bandgap fiber was designed and manufactured and a cladding-pumped fiber laser was built. A good beam quality (M^2 = 1.17) was observed at relatively high pump power. Above threshold, the slope efficiency reaches 80% as far as the absorbed pump power is considered. Neither beam degradation nor decrease of the slope for curvature radii larger than 6 cm were observed.

Experimental results show that combination of discrimination in confinement loss and overlap factors leads to selective emission of the fundamental mode. First and second modes in a 50 μm diameter core fiber could exhibit confinement loss equal to 0.03 and 4 dB/m, and overlap factors, calculated for a doped region equal to 3/5 of the core area, equal to 79% and 51%, respectively. This large difference would lead to efficient generation of a very large Gaussian beam. Increasing the core diameter leads to increased bend sensitivity (loss and field deformation). In such a case, the critical curvature radius is ~20 cm, which is still practical provided the pump absorption is high.

This research was funded by the French Research National Agency under grant ANR-06-BLAN-0091-01. D. Gaponov acknowledges the financial support of French ministère des Affaires étrangères.

References

1. V. Fomin, A. Mashkin, M. Abramov, A. Ferin, V. Gapontsev, and IPG Laser GmbH Burbach Germany, in *International Symposium on High-Power Fiber Lasers and Their Applications* (Laser Research Institute, 2006).
2. J. W. Nicholson, J. M. Fini, A. D. Yablon, P. S. Westbrook, K. Feder, and C. Headley, Opt. Lett. **32**, 2562 (2007).
3. J. P. Koplow, D. A. V. Kliner, and L. Goldberg, Opt. Lett. **25**, 442 (2000).
4. P. Wang, L. J. Cooper, J. K. Sahu, and W. A. Clarkson, Opt. Lett. **31**, 226 (2006).
5. C.-H. Liu, G. Chang, N. Litchinister, D. Guertin, N. Jacobson, K. Tankala, and A. Galvanauskas, in *Conference on Lasers and Electro-Optics/Quantum Electronics and Laser Science Conference and Photonic Applications Systems Technologies*, OSA Technical Digest Series (CD) (Optical Society of America, 2007), paper CTuBB3.
6. Y. Chen, T. McComb, V. Sudesh, M. Richardson, and M. Bass, Opt. Lett. **32**, 2505 (2007).
7. P. Yeh, A. Yariv, and E. Marom, J. Opt. Soc. Am. **68**, 1196 (1978).
8. S. Février, P. Viale, F. Gérôme, P. Leproux, P. Roy, J.-M. Blondy, B. Dussardier, and G. Monnom, Electron. Lett. **39**, 1240 (2003).
9. P. Laperle, C. Paré, H. Zheng, and A. Croteau, Proc. SPIE **6453**, 645308 (2007).